THE TAIL MOVEMENT OF BULL SPERMATOZOA. OBSERVATIONS AND MODEL CALCULATIONS

ROBERT RIKMENSPOEL
From the Population Council, The Rockefeller Institute, New York

ABSTRACT Detailed observations of the tail movement of non-rotating and rotating bull spermatozoa have been carried out. For rotating sperm a helical tail wave was found with a ratio of the amplitudes of the two perpendicular components of approximately 3 to 1. For both types of cells the variation of the amplitude and the phase shift of the wave as it travels from the proximal to the distal part are reported. Model calculations indicate that the stiffness of the tail originates in the fibrous sheath, which has a Young's modulus of 3×10^7 dynes/cm^2. Active contractile elements distributed continuously along the tail are found necessary to maintain the amplitude of the tail wave against damping by the fluid drag. If the longitudinal fibers are identified with the contractile elements the maximum tension to be developed by these fibers is 4×10^6 dynes/cm^2. The energy dissipated by the "active" part of the tail wave is at least approximately 70 percent of the total dissipation.

INTRODUCTION

Detailed information on the wave motion of the sperm tail is still relatively sparse. Observations have to be made from fast cinemicrographs. As the characteristic frequencies in the tail movement are from 20 to 30 CPS, more than 100 frames/sec. are needed. The additional requirements of dark field illumination of the specimen and short exposure time ($\approx$100 μsec.) of each frame represent technical difficulties which have been overcome only recently.

Reports up till now have mainly dealt with defining a frequency and amplitude of the tail wave, and relating these quantities to the forward velocity of the cell. It had been predicted from hydrodynamical considerations by Taylor (1952), and later by Gray and Hancock (1955), that the forward velocity due to a traveling wave in a sperm flagellum, is zero to first approximation. In second order approximation a non-zero forward velocity, v, is found, which can be expressed as

$$v \propto \frac{fb^2}{\lambda} \tag{1}$$

where f is the frequency, b the amplitude, and λ the wavelength of the tail wave. Taylor (1952) also derived that in the case in which a helical wave travels along the tail, a torque is developed, which would make the cell rotate along its longitudinal axis with a frequency proportional to the forward velocity.

Gray (1955) studied the tail movement of sea urchin spermatozoa with a multiple exposure photographic technique, using an electronic flash bulb. He found that the amplitude of the tail wave of these sperm increased from the proximal towards the distal end of the tail. Using the *average* values of b, f, and λ for 89 cells, a velocity average was calculated with the aid of equation (1) and the proportionality constant derived by Gray and Hancock (1955). The calculated velocity was found to be very close to the average of the observed velocities. No relation between b, f, λ, and v for the individual cells was reported however.

Rikmenspoel (1957*b*) with others (1960) measured the movement of bull spermatozoa from dark field cinemicrographs taken at 50 frames/sec. It was found that mainly two types of movement existed. The normal movement was characterized by a helical tail wave, accompanied by a rotation of the cell along its longitudinal axis. The rotation was observed from the periodic changes in light scattering of the head of the sperm. The frequency of rotation was found to be proportional to the forward velocity of the cell, in agreement with the prediction of Taylor. The rotation of the cell obscured the waving motion of the tail precluding measurement of its frequency. Estimates of the amplitude of the wave demonstrated a quadratic relation with the velocity of the cell, in accordance with equation (1).

The second, pathological type of movement was described by Rikmenspoel *et al.* (1960) as having a flat (2 dimensional) tail wave with no rotation. For these pathological cells, estimates of f, b, and λ were obtained. The frequency and wavelength of the wave showed no correlation with the velocity of the cell. The amplitude was related quadratically to the velocity, as for the normal movement. Velocities calculated with equation (1), using Gray and Hancock's proportionality constant, were a factor 5 higher than the observed velocities, however.

Gray in 1958, using the same method as in his earlier paper on sea urchin sperm, reported observations on bull spermatozoa. A tail wave frequency of 4 to 14 CPS was mentioned. It will be shown in the Description of the Tail Wave section of this paper, however, that this frequency does not represent the tail wave, but a beat frequency between the tail wave and the rotation of the cell. The amplitude of the wave was found to increase as the wave traveled distally along the tail, in accordance with the observations on sea urchin sperm, and with those of Rikmenspoel on bull sperm. Gray found no correlation of f, λ, or b with v.

Summarizing the foregoing, it can be said that qualitatively the phenomenology and the hydrodynamic aspects of the sperm movement are understood. A much more complete description, especially of the rotating, normal movement, is needed. However, as forward movement has been shown to be only a second order effect

a search for quantitative agreement between observations and theory would not seem especially promising.

A precise description of the *form* of the tail wave can provide information about the elastic properties of the tail. Machin (1958) has done calculations on models, in which the tail was represented by a thin, uniform, elastic rod, in which flexural vibrations are induced at one end. As only small amplitudes of vibration were considered, and the fact that an actual sperm tail is tapered was not taken into account, the results of these calculations were qualitative. It was shown, however, that propagated waves are heavily damped toward the free (distal) part of the rod. As observations till now all point to an increasing amplitude towards the distal part of the tail, this necessitates the supposition that active contractile elements are distributed along the length of the tail.

In this paper data are presented which describe the tail wave of a limited number of cells in detail. The results of the observations are compared with model calculations for large amplitude waves in a tapered tail. The conclusions confirm the need for assuming active contractile elements in the sperm tail, and they provide additional evidence for identifying these elements with the nine longitudinal fibers (see Fawcett, 1958) found in flagellae.

A preliminary communication of some of the results has been made recently (Rikmenspoel, 1964).

EXPERIMENTAL METHODS

Spermatoza were obtained from Frisian bulls at the experimental farm of the Research Institute for Animal Husbandry at de Bilt, Holland. After collection the semen was diluted 50 to 100 times and cooled to 4°C, as described before (Rikmenspoel, 1957*a*). The diluent consisted of a Na citrate solution (28 gm/liter) to which 10 per cent egg yolk was added. The diluent had been made optically clear by ultra centrifugation and filtration (Rikmenspoel, 1957*a*). For motility observations the diluted semen was warmed to 37°C. The pH of the medium was 6.7. The data reported were taken on sperm within 8 hours after collection.

As the egg yoke used in the diluent contains approximately 0.7 per cent of glucose (Romanoff and Romanoff, 1949) sufficient substrate was present in the sperm suspension.

Cinemicrographs of the sperm were made under dark field illumination, at 200 frames/second. The apparatus used incorporated an electronic flashlamp, giving an exposure of $\approx$ 150 μsec. per frame. A full description was previously published (Eykhout and Rikmenspoel, 1960).

The films were viewed and a number of cells (6 non-rotating and 10 rotating) were selected for detailed measurement. The cells were chosen to be free of interference by other nearby cells.

For each of the selected cells 50 to 70 consecutive frames were rephotographed 10× enlarged on 35 mm film. An example of such a photograph is shown in Fig. 1.

The 35 mm film was projected in an enlarger and the cell was drawn on a sheet of paper. Little spots of dirt which were fixed to the slide (as visible in Fig. 1) served as frame of reference. In this way up to 70 successive positions of the cell, observed at 5 msec. intervals were obtained.

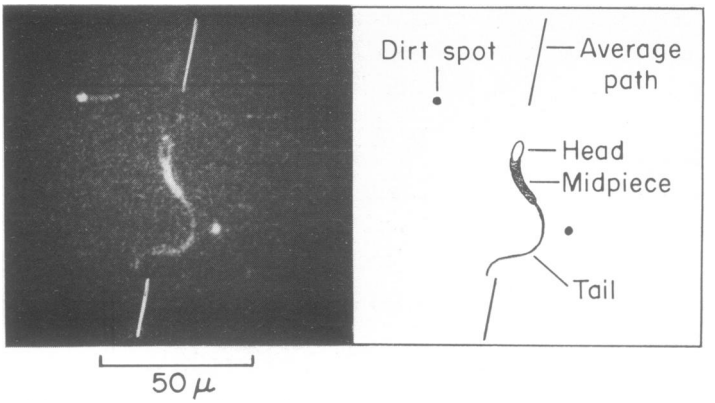

FIGURE 1 Enlarged reproduction of a part of a frame of the cinemicrographs, showing a rotating sperm. The average path along which the cell was moving is shown in the figure. The diagram at the left indicates the location of the head, midpiece, and tail of the sperm.

The "average path" along which the cell was swimming was determined by superimposing every 5th image, and drawing a line visually estimated to be the center.

On each cell 6 points were selected: the junction of the head to the midpiece, the midpiece-tail junction, and 4 points representing successive 10μ displacements along the tail. For each of the six points the deviation from the average path was measured as illustrated in Fig. 2, and plotted as a function of time. For each of the six points the projection of the transversal movement *versus* time is obtained in this way.

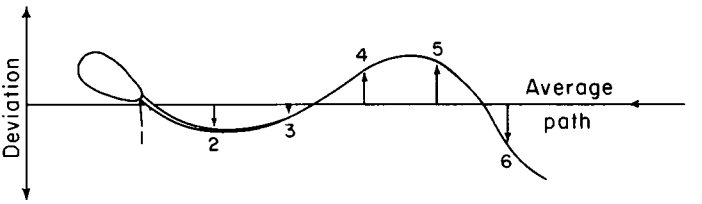

FIGURE 2 Diagram showing the way wave patterns are measured. At the six numbered points, which are to be thought of as fixed to the tail, the deviation from the average path is measured as a function of time.

Corrections for systematic deviation from the originally estimated average path, and for curvature of this path were made by drawing the average median for each curve, and replotting the curves as the distance from this corrected median. The data presented in the next section are obtained from these corrected curves.

DESCRIPTION OF THE TAIL WAVE

In this section experimental data on 10 rotating and 6 non-rotating cells are reported. Even though the non-rotating cells are recognized as pathological, they will be presented first, in view of the greater simplicity of their movement.

Non-Rotating Cells. Fig. 3 shows a typical example of the data obtained from a non-rotating sperm. It can be seen that each point of the tail executes an almost purely sinusoidal vibration around a median position. The traveling of the wave along the tail is shown by the progressive phase shift of the pattern towards the distal point.

The displacement U of each point can be written as

$$U = A(x) \sin [\omega t + \alpha(x)] \tag{2}$$

where x = distance from the proximal end of the tail (point 2 in Fig. 2) and $\omega = 2\pi f$.

Figs. 4 and 5 present the values obtained for $A(x)$ and $\alpha(x)$ on the 6 cells measured. At the distal part of the tail the quality of the data (compare Fig. 3) is less satisfactory, but fair values for $A(x)$ and $\alpha(x)$ are obtained. It can be seen in Fig. 4 that $A(x)$ increases with x. As the characteristic amplitude b for a cell, the value of $A(x)$ at $x = 20\mu$ can be taken.

Fig. 5 shows that the wave travels with decreasing speed towards the distal end. By extrapolating to $x = 50\mu$ the average line drawn in Fig. 5, it can be seen that just about one full wave is accommodated in the tail.

Table I gives the observed values for the velocity, the frequency, the characteristic amplitude, and the length of the first half wave (the value of x for $\alpha(x) = \pi$).

Rotating Cells. Fig. 6 shows a typical example of the waving motion observed on the tail of a rotating cell. The picture is strikingly different from that for the non-rotating cells.

The data are not as good towards the distal end. At the point marked number 6, the tail is often invisible on the films as it has moved far out of focus. The transversal movement of the head of the sperm (point number 1) has an amplitude of only a few microns, as was also observed in the non-rotating cells.

The rotation of the cells shows on the films by the characteristic change in light scattering off the head; whenever the head is in a position perpendicular to the plane of the slide an intense flash of light (due to specular reflexion of the light beams of the dark field illumination) is seen. The rotation frequency is obtained from these flashes.

The tail motion as seen at the points 2 through 5 of Fig. 6 can be written as a summation of two sinusoidal functions:

$$U = C_1 \sin (2\pi\nu_1 t + \delta_1) + C_2 \sin (2\pi\nu_2 t + \delta_2) \tag{3}$$

where the subscript 1 indicates the main (slowest) component and subscript 2 the faster one. By measuring the time between maxima occurring in U, estimates of ν_1 and ν_2 are obtained. It was found (Rikmenspoel, 1964) that $(\nu_2 - \nu_1)/2$ has a close correlation with the rotation frequency f_{rot}. This shows that the observed patterns are the result of a vibrational motion modulated by the rotation. From a preliminary

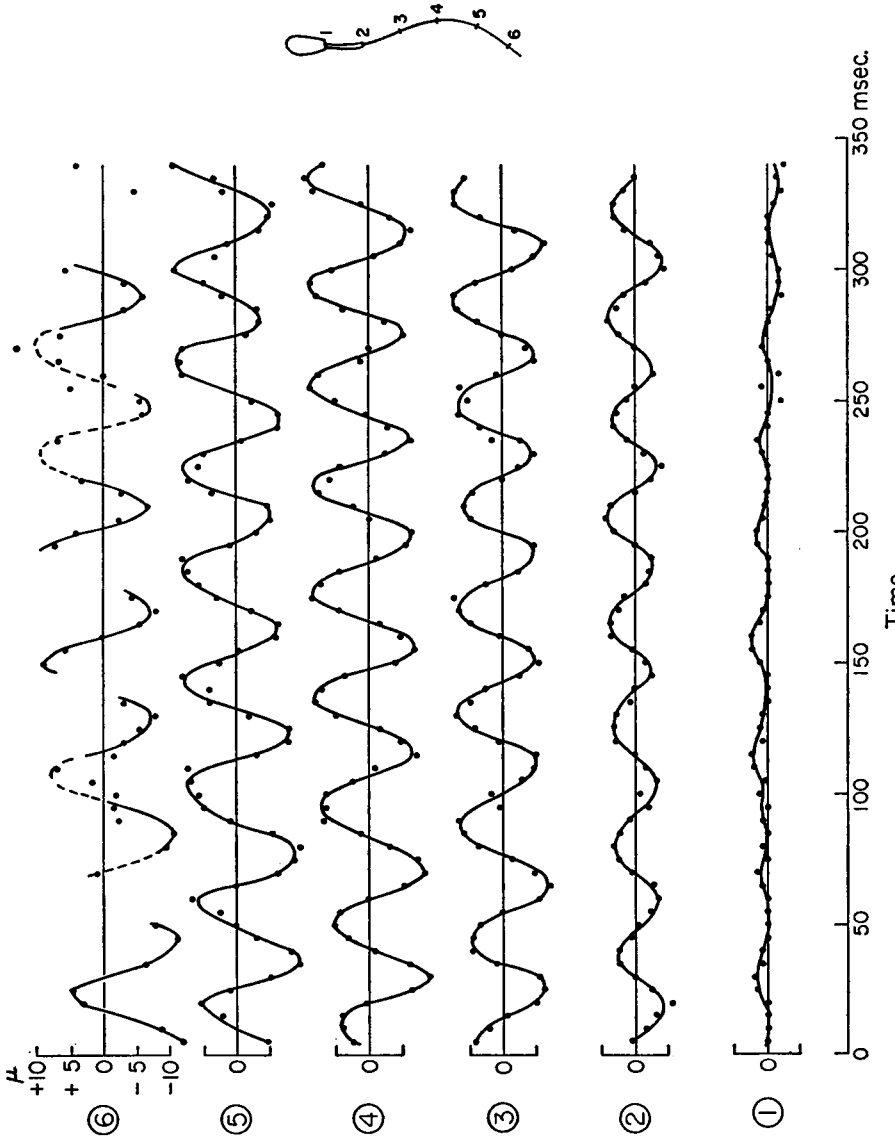

FIGURE 3 Deviation from the median position for six points on the tail of a non-rotating sperm, as a function of time. Each point describes a simple harmonic vibration around the equilibrium position (Courtesy of the New York Academy of Science).

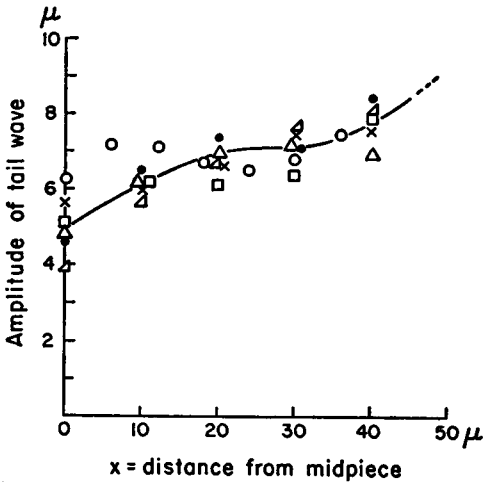

FIGURE 4 Amplitude $A(x)$ of the tail wave as a function of the distance from the midpiece for six non-rotating sperm.

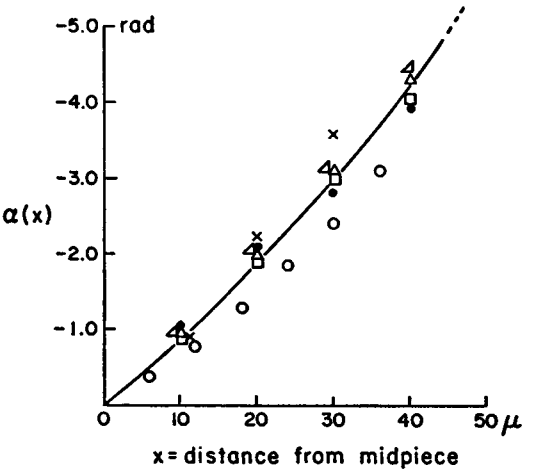

FIGURE 5 Phase angle $\alpha(x)$ of the vibration of the tail of each of six non-rotating sperm as a function of the position on the tail. $\alpha(0)$ is normalized to zero for all cells.

graphical analysis it was found that the ratio C_1/C_2 for the observed patterns was between 2:1 and 3:1.

The two above mentioned observations allow one to interpret the observed patterns. If the tail wave were a flat wave $a(x)\sin[\omega_t t + \alpha(x)]$, (with $a(x)$ = the amplitude, x = the distance from the proximal end of the tail and $\omega_t = 2\pi \times$ the wave frequency) in a plane which rotates at a speed ω_r, giving it an angular displacement $[\omega_r t + \varphi(x)]$, the patterns shown in Fig. 6 would have the form

$$U(x, t) = a(x) \sin [\omega_t t + \alpha(x)] \cos [\omega_r t + \varphi(x)]$$

TABLE I

FORWARD VELOCITY v, TAIL WAVE FREQUENCY f_t CHARACTERISTIC AMPLITUDE b, AND LENGTH $\lambda/2$ OF FIRST HALF WAVE FOR SIX NON-ROTATING SPERM

Cell	v	f_t	b	$\lambda/2$
No.	μ/sec	CPS	μ	μ
1	60	21	7.0	31
2	70	32	6.1	29
3	77	25	6.7	29
4	80	17	6.6	36
5	82	24	7.4	32
6	105	24	6.6	27

or

$$U(x, t) = \frac{a(x)}{2} \{\sin [(\omega_t + \omega_r)t + \alpha(x) + \varphi(x)] + \sin [(\omega_t - \omega_r)t + \alpha(x) - \varphi(x)]\} \quad (4)$$

in which two frequencies occur, but the amplitudes connected to them are equal.

A purely helical wave consisting of two perpendicular components with amplitude $b(x)$ and $\pi/2$ shifted in phase, gives rise to, (in a cell rotating at angular speed ω_r):

$$U(x, t) = \mathrm{b}(x) \sin [(\omega_t - \omega_r)t + \alpha(x) - \varphi(x)] \quad (5)$$

in which only one frequency occurs.

The observed phenomenon is obviously a combination of the two, this is a helical wave with unequal amplitudes of the two components. Summing equations (4) and (5), which is allowed as the phase angles have been inserted properly, gives:

$$U(x, t) = \frac{a(x) + 2b(x)}{2} \sin [(\omega_t - \omega_r)t + \alpha(x) - \varphi(x)] + \frac{a(x)}{2} \sin [\omega_t + \omega_r)t + \alpha(x) + \varphi(x)] \quad (6)$$

Comparing equations (3) and (6) then yields for the amplitudes $A_1(x)$ and $A_2(x)$ of the two components of the wave in an actual sperm:

$$A_1 = a(x) + b(x) = C_1 + C_2 \quad (7)$$

$$A_2 = b(x) = C_1 - C_2 \quad (7a)$$

The frequency of the tail wave f_{tail} and of the rotation f_{rot} are found as

$$f_{\text{tail}} = \frac{\omega_t}{2\pi} = \frac{\nu_1 + \nu_2}{2} \quad (8)$$

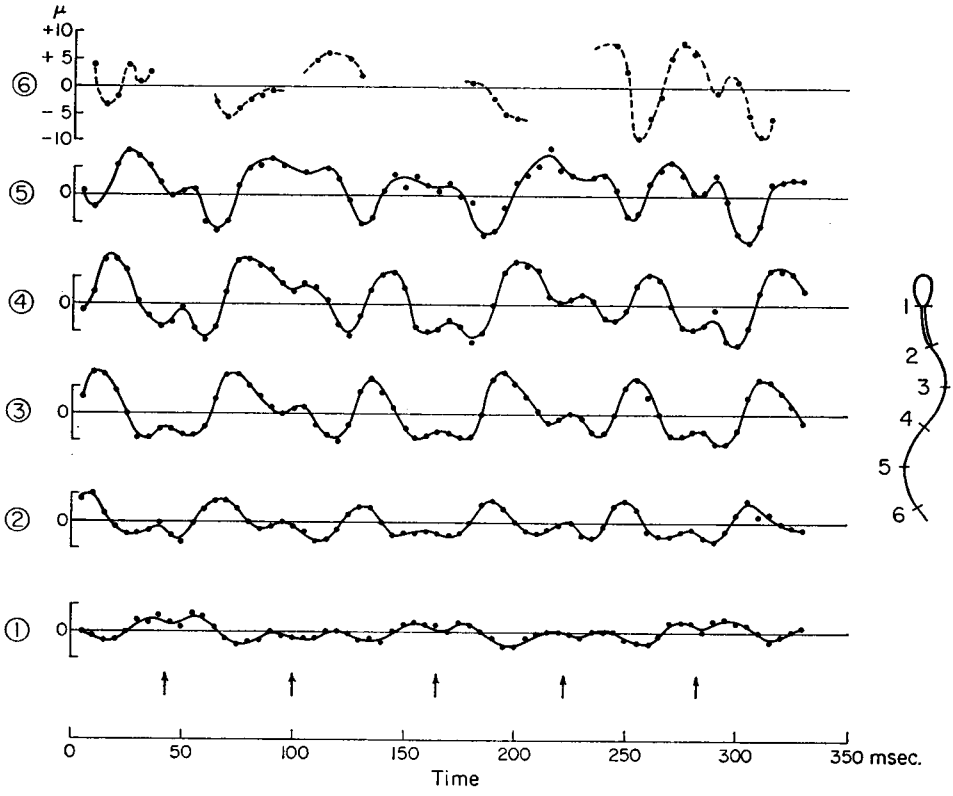

FIGURE 6 Wave patterns at six points on the tail of a rotating sperm. Each point has an apparent movement around the equilibrium position which is the sum of two vibrations (Courtesy of the New York Academy of Science). The arrows indicate the moments a light flash off the head was observed, indicating that the head was in a position perpendicular to the plane of the slide.

$$f_{rot} = \frac{\omega_r}{2\pi} = \frac{\nu_2 - \nu_1}{2} \tag{8a}$$

The phases of tail wave and rotation are found as

$$\alpha(x) = \frac{\delta_1 + \delta_2}{2} \tag{9}$$

$$\varphi(x) = \frac{\delta_2 - \delta_1}{2} \tag{9a}$$

A least-squares fit procedure, programmed for a Univac 1107 computer, was used to obtain values for $A_1(x)$, $A_2(x)$, $\alpha(x)$, ν_1, and ν_2 for the 10 rotating cells. The procedure is described in Appendix I. For each cell the data from the points on the tail numbered 2, 3, 4, and 5 were used. The analysis employed makes it possible to judge whether all four patterns of one cell can be fitted to one pair of ν_1, ν_2 values

and shows the sensitivity of obtained values for $A_1(x)$, $A_2(x)$, and $\alpha(x)$ to variation of ν_1 and ν_2.

Values of $\varphi(x)$ cannot be obtained in this way. The analysis used defines the value of δ_1 and δ_2 congruent to a modulus π, and according to equation (9*a*) the value of $\varphi(x)$ congruent to a modulus $\pi/2$ (see Appendix I). It cannot be decided, therefore, whether the rotation at the distal part lags or precedes that at the proximal end. For this reason values for $\varphi(x)$ are not presented.

The data on one of the 10 cells measured were judged to be not good enough to attempt the least-squares analysis. For two other cells the analysis showed that it was not possible to fit all four patterns to the same set of ν_1, ν_2 values. The amplitudes and phase angles proved to be too sensitive to small variation in ν_1 and ν_2 to get meaningful values.

On the remaining seven cells the analysis was performed successfully with a good convergence to a common value for ν_1 and to a common value for ν_2 for each cell. Table II shows the values for the frequencies for these cells and also the

TABLE II

FREQUENCIES ν_1 AND ν_2 OCCURRING IN THE WAVE PATTERNS OF SEVEN ROTATING CELLS.
Forward velocity v and rotation frequency are shown also

Cell	v	ν_1	ν_2	$\frac{\nu_1+\nu_2}{2}$	$\frac{\nu_2-\nu_1}{2}$	f_{rot}
No.	μ/sec	CPS	CPS	CPS	CPS	CPS
1	77	9.2	25.5	17.3	8.2	9.2
2	96	15.0	29.9	22.0	7.0	7.7
3	99	15.3	34.6	24.0	9.6	8.5
4	102	12.8	33.0	22.9	10.1	9.5
5	106	12.5	29.7	21.1	8.6	8.4
6	108	11.5	29.6	20.8	9.1	10.2
7	111	16.5	31.3	23.9	7.4	8.3

observed rotation frequency f_{rot}. It can be seen that a close agreement exists between $(\nu_2 - \nu_1)/2$ and f_{rot}.

Fig. 7 shows the values for the amplitudes of the main component $A_1(x)$ and of the smaller component $A_2(x)$ for the seven cells as a function of x. In Fig. 7*a* the values of $A_1(x)$ at $x = 40\mu$ are estimated values obtained by multiplying $A_1(x)$ at $x = 30\mu$ by the ratio of the envelopes of the patterns at $x = 40\mu$ and 30μ respectively. This was done because the data for the distal end of the tail (point number 6 in Figs. 2 and 6) are too poor to allow for a complete analysis.

Fig. 7*a* shows that towards the distal end of the tail the amplitude of the main component increases to a greater extent than does the wave amplitude of the non-rotating cells. The significance of this will be considered in the discussion.

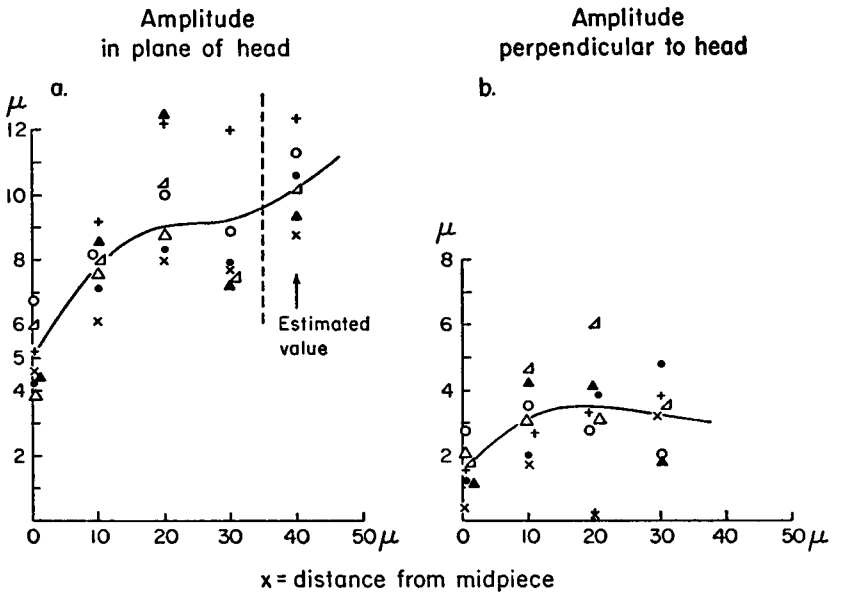

FIGURE 7 Amplitude of the tail wave of each of seven rotating sperm in the plane of the head (left) and perpendicular to the plane of the head (right).

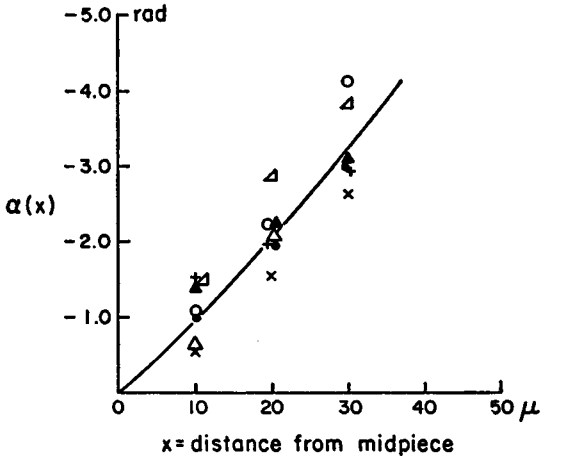

FIGURE 8 Phase angle $\alpha(x)$ of the vibration of the tail of a rotating sperm, as a function of the distance to the midpiece.

Fig. 8 shows the values for $\alpha(x)$ for the seven cells. The average curve drawn in the figure agrees very closely with the non-rotating cells in Fig. 5.

Discussion on Cell Movement. The data presented in the previous section on rotating sperm explain why previous attempts to measure the frequency of the tail wave have not given satisfactory results. When insufficient time resolution is

used in the observations, no results are obtained (Rikmenspoel *et al.*, 1960), or the "main" frequency such as that occurring in Fig. 6 is mistaken for the tail wave frequency (Gray, 1958).

Results reported here are too few and over too small a range to permit conclusions as to the validity of relations between v, f, b, and λ. The author has previously reported (Rikmenspoel *et al.*, 1960) from estimates of the amplitudes, b, of the tail wave obtained from films with 50 frames/sec., a relation with the forward velocity, v:

$$v = \varepsilon b^2 \tag{10}$$

with an average value for rotating cells of $\varepsilon_{rot} = 1.2\mu^{-1}$ sec.$^{-1}$ and for non-rotating cells $\varepsilon_{nr} = 0.8\mu^{-1}$ sec.$^{-1}$.

A characteristic amplitude for the non-rotating cells presented here is the value of $A(x)$ at $x = 20\mu$. For the rotating cells the value of $A_1(x)$ at $x = 20\mu$ of equation (7) would correspond to b in equation (10). The data in Figs. 4 and 7 and Tables I and II, then, give as average values: $\varepsilon_{rot} = 1.1 \pm 0.3\mu^{-1}$ sec.$^{-1}$ (SD) and $\varepsilon_{nr} = 1.6 \pm 0.3\mu^{-1}$ sec.$^{-1}$ (SD). The value reported here for ε_{rot} agrees satisfactorily with the earlier figure. It cannot be decided whether the apparent disagreement between the value presently found for ε_{nr} and the one previously found is due to the more accurate way of obtaining the present figure, or is due to the very small sample (6 cells) from which it was obtained. It is clear that many more data are needed before a good quantitative relation between amplitude and frequency of the wave and forward velocity can be established. A relation of this kind is very desirable for comparison of measurements of the energy production of sperm with measurements of velocities (Rikmenspoel, 1965).

MODEL CALCULATIONS

General Considerations. This section will consider what conclusions regarding the elastic properties of the tail can be drawn from the data presented in the previous section.

If the sperm tail is considered to be a thin rod, the bending moment, M, due to elastic resistance to bending of the tail can be written as:

$$M = \frac{\partial^2 U}{\partial x^2} IE \tag{11}$$

where U = deviation from the equilibrium position (see Fig. 9)
x = distance from the proximal end
I = "moment" of the cross-section of the rod relative to its median plane[1]
E = Young's modulus of the rod.

[1] The "moment" I is the quantity occurring in the theory of bending of beams, and is defined as $I = \int y^2 ds$, where ds is an infinitesimal surface element in the cross-section, and y the distance of ds from the median plane.

At the very low Reynold's number of the sperm tail movement, inertia forces can be neglected, and the counteracting moment is caused only by fluid drag. For the second derivative of this moment it holds (compare Sommerfeld, 1947):

$$\frac{\partial^2 M}{\partial x^2} = -C_n \frac{\partial U}{\partial t} \tag{12}$$

where C_n = drag coefficient for movement of the tail normal to its median axis.

Equations (11) and (12) combine to the differential equation for a passive tail:

$$\frac{\partial^2}{\partial x^2}\left[IE \frac{\partial^2 U}{\partial x^2}\right] = -C_n \frac{\partial U}{\partial t} \tag{13}$$

Machin (1958) has calculated the behavior of such a passive tail using as boundary conditions free movement at the distal end ($\partial^2 U/\partial x^2 = \partial^3 U/\partial x^3 = 0$), and at the proximal end: $U = 0$, $\partial U/\partial x = B \sin \omega t$. The value for C_n given by Hancock (1953) was adopted:

$$C_n = \frac{4\pi\eta}{-0.5 + \ln (2\lambda/\rho)} \tag{14}$$

where η = viscosity of the fluid

ρ = radius of the cross-section of the tail.

The solutions obtained by Machin are valid for small amplitude.

In order to arrive at solutions allowing for quantitative comparison with the observed motion it is necessary to make two refinements in equation (13):

(*a*) The taper of the tail has to be taken into account. The diameter of the tail of bull spermatozoa at the distal end is given by Bretschneider (1947) as 0.55× the diameter at the proximal end. For our model we have assumed the tail to be a cut-off conic as shown in Fig. 9. In the notion of Fig. 9, it can be written

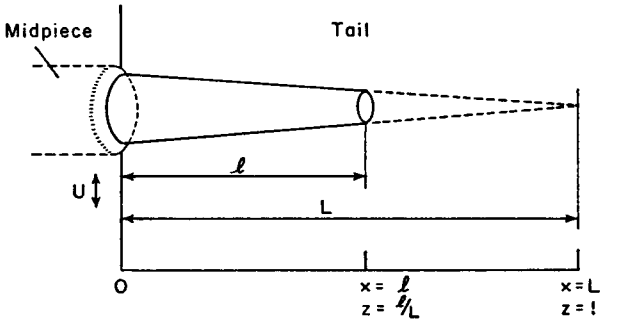

FIGURE 9 Diagram illustrating the model of the sperm tail used in the calculations. The dimensions in the direction of U are greatly exaggerated.

$$I = I_0 \frac{(L - x)^4}{L^4} \tag{15}$$

where I_0 is the "moment" relative to the median plane of the tail at $x = 0$.

(*b*) When the amplitude of the wave is not small, as is the case in an actual sperm, the drag force which dampens the tail wave is no longer normal to the tail. As an approximation can be taken for the dragforce, dF, on a tail segment (γ is the angle between the tail segment and the x axis):

$$dF = -C_n \frac{\partial U}{\partial t} \cos \gamma \tag{16}$$

One can write

$$\cos \gamma = \left[1 + \left(\frac{\partial U}{\partial x}\right)^2\right]^{-1/2} \approx 1 - \tfrac{1}{2}\left(\frac{\partial U}{\partial x}\right)^2 \tag{17}$$

From equation (2) follows for $\partial U/\partial x$ in an actual sperm:

$$\begin{aligned} \frac{\partial U}{\partial x} &= A'(x) \sin [\omega t + \alpha(x)] + A(x)\alpha'(x) \cos[\omega t + \alpha(x)] \\ &= B(x) \cos [\omega t + \alpha(x) + \beta(x)] \end{aligned} \tag{18}$$

with

$$B(x) = -\sqrt{[A(x)\alpha'(x)]^2 + [A'(x)]^2} \tag{19}$$

$$\beta(x) = \operatorname{arctg}\left[-\frac{A'(x)}{A(x)\alpha'(x)}\right] \tag{20}$$

An evaluation of $\beta(x)$ of equation (20), made from the data given in the previous section, shows that $\beta(x)$ is small. This means that the correction factor $\cos\gamma$ is almost in phase with $\partial U/\partial t$, and can be replaced by

$$\cos \gamma \approx 1 - \tfrac{1}{2}[B(x)]^2 \tag{21}$$

Fig. 10 shows an evaluation of the correction factor with the aid of the data from the observation on rotating and non-rotating cells. The corrected drag coefficient $C_n\{1 - \tfrac{1}{2}[B(x)]^2\}$ is also shown for a tapered tail in Fig. 10. In order to facilitate

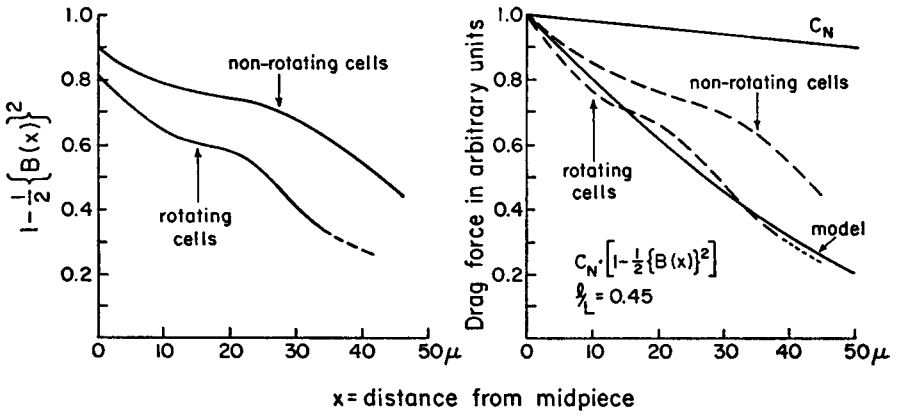

FIGURE 10 Correction factor for the drag coefficient (left) for rotating and non-rotating cells. The right side shows the actual value for the drag coefficient in a tapered tail.

computations the drag coefficient to be inserted in equation (13) has been written as (the notation $k(x)$ is used to distinguish it as a model approximation):

$$k(x) = k_0 \frac{(L - x)^2}{L^2} \tag{22}$$

Equations (15) and (22) give for the differential equation of our model

$$\frac{\partial^2}{\partial x^2}\left[(L - x)^4 \frac{\partial^2 U}{\partial x^2}\right] = -\frac{k_0 L^2}{I_0 E}(L - x)^2 \frac{\partial U}{\partial t} \tag{23}$$

Equation (23) can be made dimensionless (except for U) with $z = x/L$ and $\tau = \omega t$:

$$\frac{\partial^2}{\partial z^2}\left[(1 - z)^4 \frac{\partial^2 U}{\partial z^2}\right] = -c\left(\frac{L}{l}\right)^4 (1 - z)^2 \frac{\partial U}{\partial \tau} \tag{24}$$

with

$$c = \frac{k_0 \omega l^4}{I_0 E} \tag{25}$$

As boundary conditions for equation (24) were used $\partial^2 U/\partial z^2 = \partial^3 U/\partial z^3 = 0$ at $z = l/L$. At $z = 0$ can be written $U = A(0)\sin\tau$. For both the rotating and the non-rotating cells the observed average value of $A(0)$ was 5μ (Figs. 4 and 7). At $z = 0$ it holds also [compare equations (18) through (20)]: $\partial U/\partial z = L \cdot \partial U/\partial x = L \cdot B(0)\cos[\tau + \beta(0)]$.

From the average of the experimental data, shown in Figs. 4, 5, 7, and 8, an evaluation of $B(0)$ and $\beta(0)$ gives for the rotating cells $B(0) = -0.55$, $\beta(0) = 0.4$ rad. For the non-rotating cells $B(0) = -0.5$ and $\beta(0) = 0.25$ rad.

Solutions for equation (24) with the described boundary conditions have been computed on a IBM 7094 computer with the method described in Appendix II. The value of c in equation (25) was varied through a wide range. For l/L, the taper of the tail, the values 0.35, 0.45, and 0.65 were used. It should be kept in mind that these different values for l/L should not be interpreted as having an exact geometrical meaning, but that each represents a different way in which the ratio of viscous to elastic forces varies from the proximal to the distal end.

The solutions for equation (24), transformed back to be expressed as functions of $x(=L \cdot z)$ necessarily have the form $U = A(x)\sin[\tau + \alpha(x)]$. In order to arrive at values for c and l/L which are valid for an actual sperm, $A(x)$ or $\alpha(x)$ has to be fitted to the observed values. $A(x)$, the way the amplitude changes as the wave travels along the tail, is not suitable for this purpose as its form will depend strongly on whether active contractile elements are present in the tail.

However, Machin (1963) has shown that in case active elements are present in the tail a suppression of "unwanted" induced modes occurs, and only enhancement of the initiating wave remains (see also the discussion). This means that solutions of

equation (24) at a given c and l/L will be approximately in phase with solutions at the same c and l/L, but with the addition of active contractile elements. Fitting the calculated $\alpha(x)$ to the observed one has, therefore, been taken as a valid procedure in order to obtain values for c and l/L, which are applicable to an actual sperm. Of the parameters that constitute the constant c [see equation (25)], good values for k_0 and l are available. Thus, the information to be derived is a value for I_0E, the "bending resistance" of the tail.

The Bending Resistance of the Tail. The shape of the curve for $\alpha(x)$, as computed for various values of c and for $l/L = 0.45$ is shown in Fig. 11. As is explained in Appendix II, $\alpha(x)$ is insensitive to small variations in $B(0)$ and $\beta(0)$. The computations were, therefore, performed only with one set of values: $B(0) = -0.50$, $\beta(0) = 0.25$. The slope of $\alpha(x)$ at $x = 0$ depends only on the

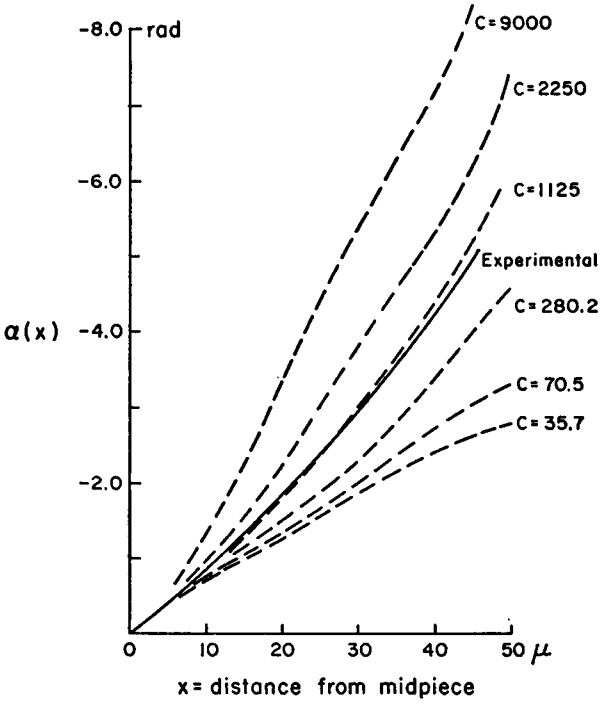

FIGURE 11 Computed form of $\alpha(x)$ for various values of the stiffness of the tail.

boundary conditions (see Appendix II) and is, therefore, the same for all curves shown. At a value of $c = 1.1 \times 10^3$ the computed curve fits well to the average of the experimental data.

The influence of variation of the taper, l/L, has to be investigated. A convenient way of presenting this is to plot that value of x where $\alpha(x) = \pi$ (length of first half

wave) and where $\alpha(x) = 2\pi$ (length of first full wave) as a function of c. Fig. 12 shows these data computed for three values of l/L. Inserted in Fig. 12 are points showing the observed values for the length of the first half wave of rotating and non-rotating cells, as a function of ω. This set of points together with the ω-axis is shifted horizontally in Fig. 12 such that the best fit with the computed values is obtained. It can be observed in Fig. 12 that the influence of the taper l/L on the length of the first half wave is smaller than the spread in the experimental data. In view of the fact that an extrapolation of the data of Fig. 5 shows that just one full wave is present in the tail, the values adopted as best for actual sperm are $l/L = 0.45$ and

$$\frac{c}{\omega} = \frac{k_0 l^4}{I_0 E} = 7.2(\text{seconds}) \tag{26}$$

Of the quantities in equation (26), l can be taken to be 50μ. The drag coefficient at the proximal junction of the tail, k_0, may be taken to be equal to C_n of equation (14). With $\rho = 0.2\mu$ (Bahr and Zeitler, 1964) and $\eta = 10^{-2}$ poise (Rikmenspoel, 1957*b*), $k_0 = 2.1 \times 10^{-2}$ dyne cm^{-2} sec. This gives for the bending resistance at the proximal junction:

$$I_0 E = 1.8 \times 10^{-12} \text{ dyne cm}^2 \tag{27}$$

Many details are known about the inner structure of the sperm tail. The tail is known to contain 9 longitudinal fibers (plus 2 central fibers), embedded in matrix, and surrounded by a fibrous sheath. From electron micrographs of Fawcett (1958) and Rothschild (1962), a cross-section of the tail of a bull sperm at the proximal junction can be deduced as illustrated in Fig. 13.

I_0 in equation (27) depends only on geometric considerations. For the three different structures in the cross-section of the tail of Fig. 13, the value of I_0 can be calculated as: fibrous sheath $I_0 \approx 6 \times 10^{-20}$ cm^4, longitudinal fibers $I_0 \approx 4 \times 10^{-21}$ cm^4, matrix $I_0 \approx 4 \times 10^{-21}$ cm^4. If the rigidity of the tail were caused by anyone of these three structures alone, the values for the Young's modulus would be:

$$\begin{aligned} \text{sheath alone:} &\quad E \approx 3 \times 10^7 \text{ dyne/cm}^2 \\ \text{fibers alone:} &\quad E \approx 4.5 \times 10^8 \text{ dyne/cm}^2 \\ \text{matrix alone:} &\quad E \approx 4.5 \times 10^8 \text{ dyne/cm}^2. \end{aligned}$$

Table III presents values in the literature for Young's modulus of some biological tissues. It is clear by comparison with the above mentioned figures that the longitudinal fibers and the matrix would have to possess unrealistically high values of E in order to make an appreciable contribution to the stiffness of the sperm tail.

It can safely be concluded that the stiffness of the tail is caused by the sheath

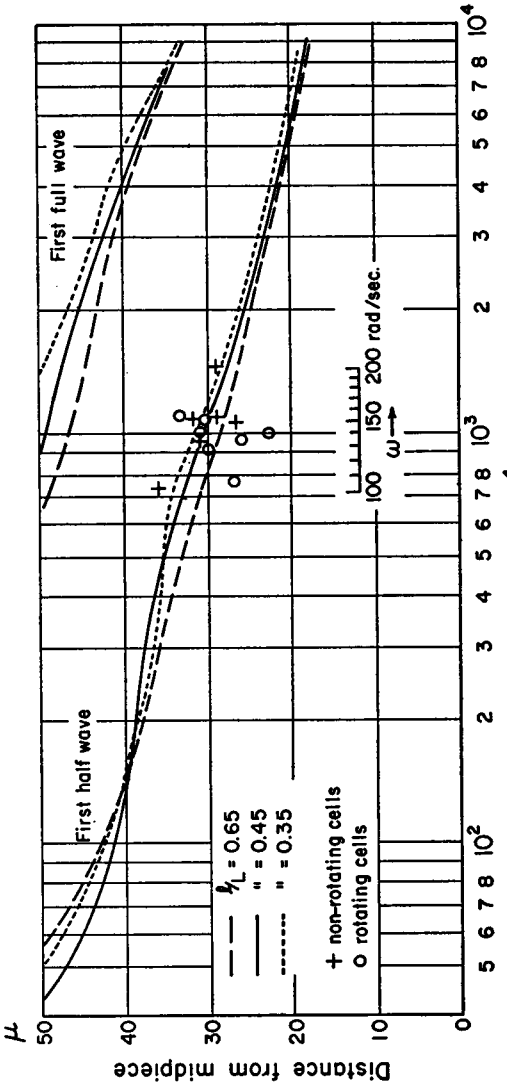

FIGURE 12 Length of first half wave and of the first full wave, computed as the function of the stiffness of the tail at three values of the taper $1/L$. The crosses and circles represent measured data.

which is probably a collagen like material with $E \approx 3 \times 10^7$dyne/cm^2. This agrees well with the fibrous nature of the sheath.

Bending Moments in the Sperm Tail. With the values of I_0E and l/L for the tail of a bull sperm derived in the previous section, a "passive" wave induced at the proximal end dampens out as it progresses towards the distal end of the tail.

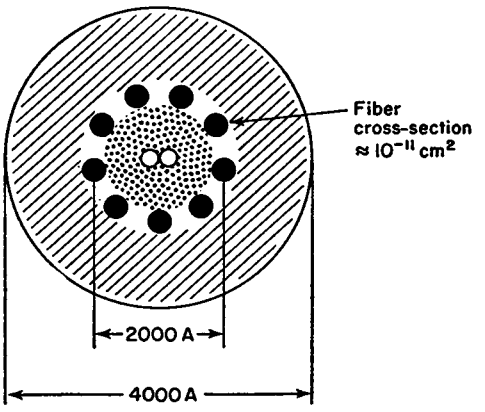

FIGURE 13 Diagram of a cross-section of a bull sperm tail at the proximal junction. The cross hatched area represents the fibrous sheath, the dotted area the matrix. The nine peripheral fibers are shown as the black circles.

TABLE III

YOUNG'S MODULUS E OF SOME BIOLOGICAL TISSUES

Tissue	E	Reference
	dyne/cm²	
Collagen (3% strain)	3×10^7	Meyer and Ferri, 1936
Elastin	1×10^7	" " " "
Extracted muscle fibers	6×10^7	Bozler, 1957

Fig. 14 shows the computed value of $A(x)$ for $c = 1125$ and $l/L = 0.45$. It is clear that in order to account for the actually observed form of $A(x)$ it is necessary to assume active contractile elements distributed along the tail. This is in agreement with the findings of Machin (1958).

A distribution of "active" bending moments M_{act} (x, t) can be inserted in the right-hand side of equation (11). Taking into account the taper, and after the transformation $z = x/L$ and $\tau = \omega t$, M_{act} can be expressed as:

$$M_{act} = (1 - z)^4 m_{act}(z, \tau) I_0 E \tag{28}$$

Equation (28) together with equation (24) gives for an "active" tail:

$$\frac{\partial^2}{\partial z^2}\left[(1 - z)^4\left(\frac{\partial^2 U}{\partial z^2} + m_{act}\right)\right] = -c\left(\frac{L}{l}\right)^4 (1 - z)^2 \frac{\partial U}{\partial \tau} \tag{29}$$

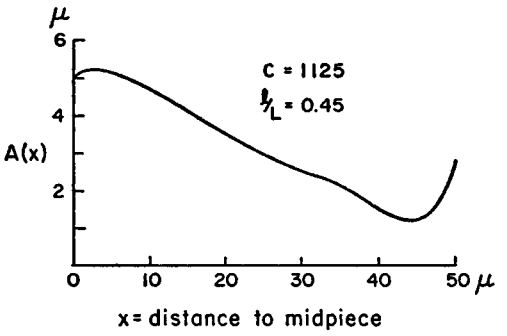

FIGURE 14 Computed form of $A(x)$ for a "passive" sperm tail. Comparison with the observed data (Figs. 4 and 7) shows that that computed wave amplitude is too small at the distal end.

The actual form of $m_{act}(z, \tau)$ is of course not known.
As a crude approximation we have used:

$$m_{act}(z, \tau) = p \frac{\partial^2 U}{\partial z^2} \tag{30}$$

The constant p in equation (30) should be understood to represent the ratio between the "active" bending moment, and the bending moment which is elastically induced due to the wave originating at the proximal end.

Using the approximation (30), equation (29) becomes

$$\frac{\partial^2}{\partial z^2}\left[(1 - z)^4 \frac{\partial^2 U}{\partial z^2}\right] = -\frac{c}{1 + p}\left(\frac{L}{l}\right)^4 (1 - z)^2 \frac{\partial U}{\partial \tau} \tag{31}$$

Equation (31) can be solved for different values of p, with the same method as was used for equation (24). It should be kept in mind, however, that if the solutions are expressed as $U = A(z)\sin[\tau + \alpha(z)]$, only $A(z)$ can be considered as having physical significance. The approximation used in equation (30) in effect permits one to ascertain the extra bending moment that has to be added in a passive tail in order to bring the amplitude of the wave up to the observed level. In an actual sperm a phase shift between m_{act} and $\partial^2 U/\partial z^2$ will have to occur (Machin, 1958), and consequently the phase $\alpha(z)$ of solutions of equation (31) cannot be taken as having quantitative value. An evaluation of p can be made by comparing the observed form of $A(z)$ for rotating and non-rotating sperm, with computed forms for various values of p. It is shown in Appendix II that in this case separate values for the boundary condition $\partial U/\partial z = L \cdot B(0)\cos[\tau + \beta(0)]$ at $z = 0$ must be employed for the two types of movement. The actual values used were mentioned earlier in this section: rotating cells, $B(0) = -0.55$, $\beta(0) = 0.4$ rad; non-rotating cells, $B(0) = -0.5$, $\beta(0) = 0.25$ rad.

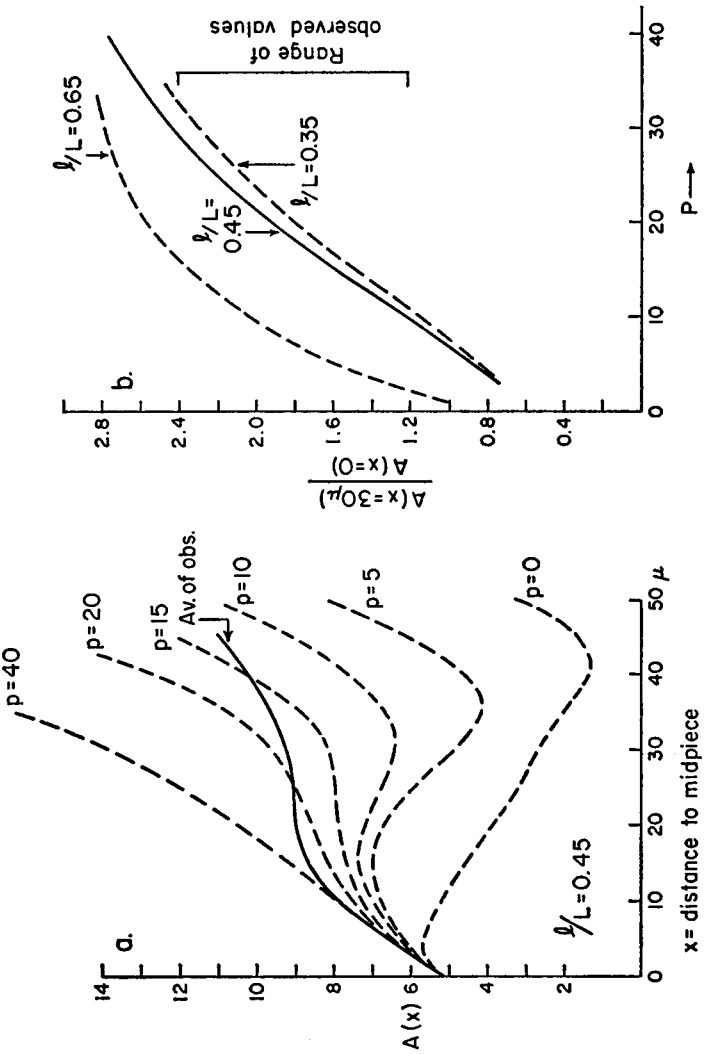

FIGURE 15 *a*. Computed form of $A(x)$ for "active" sperm tails (left). *b*. The value of the ratio $A(30)/A(0)$ as a function of p, at 3 values of the taper $1/L$. The *boundary* conditions used were those for rotating sperm.

Fig. 15*a* shows a comparison of computed forms of $A(x)$ with the average of the experimental data, for the rotating cells. In order to assess the influence of the taper l/L of the tail, the ratio $A(x = 30\mu)/A(x = 0)$ is plotted in Fig. 15*b* as a function of p, at three different values of l/L. The range of observed values of $A(x = 30\mu)/A(x = 0)$ is indicated in Fig. 15*b*.

Fig. 16*a* and *b* show the results for the non-rotating cells.

It can be seen from Figs. 15 and 16 that for both types of movement the value of p is in the order of 15. The taper l/L of the tail has no essential influence on this value. In the last 15μ of the tail, the computed amplitude at $p = 15$ is too high, which may indicate that in a real sperm the activity decreases towards the distal end of the tail. In general we can conclude, however, that almost all of the bending moment in the tail is provided by active contractile elements.

Actual values of the bending moment, M, can be readily calculated with

$$M = \frac{\partial^2 U}{\partial x^2} I_0 E \left(1 - \frac{x}{L}\right)^4. \tag{32}$$

$\partial^2 U/\partial x^2$ for rotating sperm can be evaluated from the average curves presented in Figs. 7*a* and 8. The maximum bending moment to be provided by the contractile elements at the proximal junction of a rotating cell becomes, taking $(\partial^2 U/\partial x^2)_{max} = 7 \times 10^2$ cm^{-1}, $I_0 E = 1.8 \times 10^{-12}$ dyne cm^2:

$$M_{max} = 12 \times 10^{-10} \text{ dyne cm.}$$

Assuming that this moment is produced by the four longitudinal fibers (see Fig. 13) at one side of the median plane, the force, P, needed is

$$P \approx 4 \times 10^{-5} \text{ dyne/fiber.}$$

With a cross-section, S, of 10^{-11} cm^2 of each fiber the maximum tension P/S to be developed in the fiber is:

$$P/S \approx 4 \times 10^6 \text{ dyne/cm}^2$$

This is well within the range of values for P/S for skeletal muscle reported in the literature of 1 to 5×10^6 dyne/cm^2 (Handbook of Biological Data, 1956).

Energy Dissipation by the Sperm Tail. It is of interest to compare the energy dissipation of an actual sperm with the energy dissipated by the "passive" part of the tail wave. For a non-rotating sperm one can write for the dissipation dW of a tail segment ds due to the fluid drag forces:

$$\frac{dW}{ds} = \tfrac{1}{2}\omega^2 C_n [A(x)]^2 \{1 - \tfrac{3}{4}[B(x)]^2\} \tag{33}$$

For a rotating sperm this approximation is not valid. A more accurate calculation, as was done by Carlson (1959) for a purely sinusoidal wave, is not within the scope of

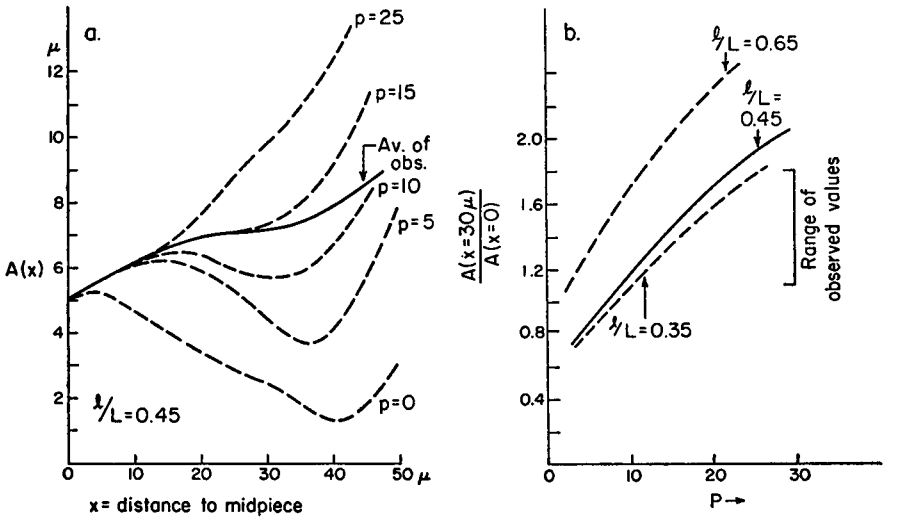

FIGURE 16 The same as Fig. 15, but for non-rotating sperm.

this paper. Rotating sperm dissipate in general more energy than the non-rotating ones due to the larger amplitude of the wave towards the distal end. Precise calculations should take into account both components of the tail wave as well as the influence of the rotation. It seems reasonable to defer these calculations until more data, covering a wider range of values of forward velocities of cells are available. The situation for rotating sperm is not essentially different from that for non-rotating sperm, however.

For our model of the tail we can write:

$$\frac{dW_{cal}}{ds} = \tfrac{1}{2}k_0\left(1 - \frac{x}{L}\right)^2 \dot{U}_m^2 \tag{34}$$

where $\dot{U}_m$ is the amplitude of the sinusoidal function $\partial U/\partial t$. Fig. 17 shows an evaluation of dW/ds obtained by inserting in equation (33) the average of the data of Figs. 4 and 5, taking $\omega = 135$ rad/sec. Also shown in Fig. 17 is the value of dW_{cal}/ds for the passive model with $l/L = 0.45$, $\omega = 135$ rad/sec. and for the "active" model at $p = 15$. Taking into consideration the approximate nature of the "active" model, the fit with the curve for the average of the observed data is surprisingly good.

By integrating dW/ds and dW_{cal}/ds over the tail, the total hydrodynamic dissipation is found. The ratio of the energy dissipation of the "passive" part W_{pass} of the wave to that of the actual wave W_{tot} is thus found

$$W_{pass} \approx 0.3\, W_{tot}$$

For the rotating cells this ratio will be even lower.

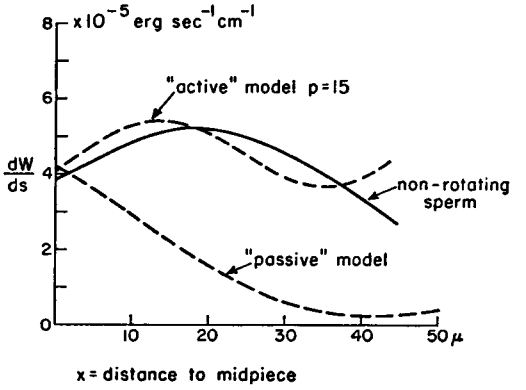

FIGURE 17 Energy dissipation by segments of the tail of a non-rotating sperm, and of our "passive" and "active" model.

DISCUSSION

The results of the model calculations in the preceding section can be considered as additional evidence for identifying the 9 longitudinal fibers in the sperm tail with active contractile elements. Burnasheva (1958) has reported properties of a contractile protein, spermosin, extracted from bull sperm, which would classify it as a myosin-like material. Myosin antibody reactivity in the rat sperm tail was found by Nelson (1961) to be concentrated in the longitudinal fibers. These two observations fit in well with the calculated maximal tension of 4×10^6 dyne/cm^2 to be developed if the fibers are the contractile elements.

By kinetic experiments, it has been shown that the motility of bull sperm is dependent on continuous energy supply (Rikmenspoel, 1965). The experiments of Hoffman-Berling (1958), Bishop (1962), and Brokaw (1962) on glycerin extracted sperm tails have shown that the immediate source of contractile energy is ATP. Nelson (1964) has found that almost 80 per cent of the ATP-ase activity of bull sperm is found in the tail, the remainder being in the midpiece. The figure reported in this paper that at least 70 per cent of the energy dissipated by the tail serves to provide the "active" contractile part of the tail wave is in good agreement with these earlier observations.

Roughly nine-tenths of the bending moment in an actual sperm tail is caused by the contractile elements in the tail. This puts strong emphasis on the necessity for mechanisms for suppressing waves modes in the tail other than those synchronized with the wave which can be assumed to be initiated in the midpiece. Machin (1963) has proposed a non-linearity of the tension-length relation in the contractile elements of the sperm tail. This was in analogy with effects observed in insect flight muscle (Machin and Pringle, 1960). In this paper it has been shown that the stiffness of the tail is most probably caused by collagen-like material in the fibrous

sheath of the tail. Collagen is known to possess a strongly non-linear strain-stress behavior (Meyer and Ferri, 1936). A non-linearity of the Young's modulus in the differential equation for the tail, can be written in the same form as the non-linearity proposed by Machin. The suppression mechanism caused by non-linear effects will, therefore, work in both cases.

The observation that the amplitude of the tail wave of rotating cells increases distally stronger than that of non-rotating cells would at first sight lead one to the conclusion that a damage of the contractile elements has occurred. However, the fact that the ratio of "active" to passive bending moments is of the same order of magnitude for the rotating and the non-rotating sperm indicates that the difference between the two types of cells is most probably not in the contractile fibers of the tail. Cold shock is one of the main causes of the pathological, non-rotating type of movement (Rikmenspoel, 1957*b*). It is known (Mann, 1964) that cold shock damages the integrity of the mitochrondria containing section (the midpiece). It seems reasonable to assume that this is accompanied by such mechanical damage that only a part of the initiating wave, which starts in the midpiece, is left over.

APPENDIX I

Equation (3) of the text can be rewritten as

$$U = C_1' \sin(2\pi\nu_1 t) + C_1'' \cos(2\pi\nu_1 t) + C_2' \sin(2\pi\nu_2 t) + C_2'' \cos(2\pi\nu_2 t).$$

We define $H = \int \{U_{obs} - U\}^2 dt$, where U_{obs} is the observed pattern (see Fig. 6). For a given pair of (ν_1, ν_2) values, $C'_1 \ldots C''_2$ can be determined by linear least-square fitting such that H is a minimum h.

For each of the four patterns of a rotating cell the values of $C'_1 \ldots C''_2$ and h were computed for 36 sets of (ν_1, ν_2). A plot of h over an area of the (ν_1, ν_2) plane was thus obtained for each of the four patterns. The lowest value h_{min} of h for one pattern defines the value of (ν_1, ν_2) for which the best fit is obtained. The best value of (ν_1, ν_2) for the whole cell was taken as the average of the four pairs, each weighed proportionally to $1/h_{min}$. For this weighed average of (ν_1, ν_2) the four sets of $C'_1 \ldots C''_2$ were interpolated from the computed values at the neighboring points in the (ν_1, ν_2) plane.

C and δ of equation (3) of the text are obtained (with the appropriate subscript) as:

$$C = \sqrt{C'^2 + C''^2}$$

$$\delta = \operatorname{artcg}(-C'/C'')$$

It should be noted that the value of δ found is congruent to a modulus π. The value of $\alpha(x)$ and $\varphi(x)$ of equation (9) of the text are thus congruent to a modulus $\pi/2$. $\alpha(x)$ can be roughly estimated from the successive phase shift of the curves of Fig. 6. To the calculated value of $\alpha(x)$ a number $n.\pi/2$ was added such that closest proximity with the estimated value was obtained.

For $\varphi(x)$ this estimation is not possible, and consequently no values are reported.

APPENDIX II

We wish to find solutions for the equation

$$\frac{\partial^2}{\partial z^2}\left((1-z)^4\frac{\partial^2 U}{\partial z^2}\right) = -c\left(\frac{L}{l}\right)^4(1-z)^2\frac{\partial U}{\partial \tau} \tag{1}$$

The boundary conditions can be rewritten as

$$U = a\sin\tau,\ \partial U/\partial z = b\cos(\tau+\beta)\text{ at } z = 0, \text{ and}$$

$$\partial^2 U/\partial z^2 = \partial^3 U/\partial z^3 = 0\text{ at } z = l/L.$$

The solutions of equation (1) can be written, using complex notation, as:

$$U = Ge^{+i\tau} + G^*e^{-i\tau} \tag{2}$$

with

$$G = \sum_{i=0}^{3}\gamma_i g_i \tag{3}$$

and where g_j $(j = 0, \ldots, 3)$ are the four independent solutions of the z-dependent part of equation (1).

The four solutions are known to be second order Bessel functions of imaginary argument (Kamke, 1948). For simplicity of computing the g_j have been developed in power series:

$$g_j = \sum_n \alpha_{j,n}z^n \tag{4}$$

For $\alpha_{j,n}$ a recurrent relation can be derived:

$$\alpha_{j,n+4} = 2\alpha_{j,n+3} - \alpha_{j,n+2} - \frac{ic(L/l)^4\alpha_{j,n}}{(n+1)(n+2)(n+3)(n+4)} \tag{5}$$

with $\alpha_{j,n} = \delta_{j,n}$ $(j, n = 0, \ldots, 3)$.

In the actual program between 250 and 500 terms were computed, depending on the value of l/L for the case. Of the coefficients with which the four solutions have to be combined in equation (3), γ_0, and γ_1 are obtained from:

$$\gamma_0 = \frac{a}{2i} \tag{6}$$

$$\gamma_1 = \frac{b}{2}e^{i\beta} \tag{6a}$$

The boundary conditions at $z = l/L$ give a set of two equations for γ_2 and γ_3:

$$\gamma_2 g_2'' + \gamma_3 g_3'' = \frac{a}{2i}g_0'' + \frac{b}{2}e^{i\beta}g_1'' \tag{7}$$

$$\gamma_2 g_2''' + \gamma_3 g_3''' = \frac{a}{2i}g_0''' + \frac{b}{2}e^{i\beta}g_1''' \tag{7a}$$

It can be seen from equations (6) to (7a) that the solutions obtained for the tail wave are not linear functions of a.

Equation (2) can be rewritten as

$$U = A(z) \sin (\tau + \alpha(z)) \tag{8}$$

with

$$A(z) = 2|G| \tag{8a}$$

$$\alpha(z) = \text{arctg } [-ReG/ImG] \tag{8b}$$

the slope $d\alpha(z)/dz$ of the curve of $\alpha(z)$ *versus* z can be written according to equation (8) and (8*b*)

$$\frac{d\alpha(z)}{dz} = -\frac{1}{|G|^2} [ReG' \cdot ImG - ReG \cdot ImG'] \tag{9}$$

For $z = 0$ it follows from equation (9) with (6) and (6*a*) that

$$\left(\frac{d\alpha(z)}{dz}\right)_{z=0} = \frac{b}{a} \cos \beta \tag{10}$$

which is independent of the stiffness of the tail. The angle β is small for both the rotating and the non-rotating cells (0.4 rad and 0.2^5 rad respectively). Cos β in equation (10) has the value 0.9 for the average of the rotating cells, 0.96 for the non-rotating cells. As a consequence, in investigating the phase $\alpha(z)$ of solutions of equation (1) the same boundary conditions can be used for both types of cells.

For the function $A(z)$ it holds:

$$\frac{dA(z)}{dz} = \frac{2}{|G|} [ReG \cdot ReG' + ImG \cdot ImG'] \tag{11}$$

At $z = 0$ equation (11), with (6) and (6*a*), gives

$$\left(\frac{dA(z)}{dz}\right)_{z=0} = -b \sin \beta$$

For the rotating cells $\sin \beta = 0.45$, for the non-rotating cells $\sin \beta = 0.25$. This difference is big enough to make it necessary to use separate boundary conditions for the two types of cells when the function A (z) is studied.

The experimental part of the work reported in this paper was performed at the Research Institute for Animal Husbandry at Zeist, Holland. The work was continued at the Johnson Foundation of the University of Pennsylvania, Philadelphia., and finished at the Laboratory of the Population Council.

The support in part by the National Institute of Health Division of Child Health and Human Development (Grant HD-1042) is gladly acknowledged.

Part of the calculations of Appendix II were done by Mr. Richard Larson whose assistance I gladly acknowledge.

I wish to thank Mrs. Rose Caputo for help with analyzing the film data.

Received for publication, January 14, 1965.

REFERENCES

BAHR, G. F., and ZEITLER, E., 1964, *J. Cell Biol.*, **21**, 175.

BISHOP, D. W., 1962, in Spermatozoan Motility, D. W. Bishop editor, Washington, D. C., American Association for the Advancement of Science.

BOZLER, E., 1957, in Tissue Elasticity, J. W. Remington editor, Washington, D. C., American Physiol. Society.

BRETSCHNEIDER, L. H., and VAN ITERSON, W., 1947, *Proc. Koninkl. Ned. Akad. Wetenschap.*, **50**, 88.

BROKAW, 1962, in Spermatozoan Motility, D. W. BISHOP, editor, Washington, D. C., American Association for the Advancement of Science.

BURNASHEVA, S. A., 1958, *Biokhimiya*, **23**, 558.

CARLSON, F. D., 1959, *Proc. Nat. Biophysics Conf.*, 443.

EYKHOUT, P., and RIKMENSPOEL, R., 1960, Research Film **3**, 304.

FAWCETT, D. W., 1958, *Internat. Rev. Cytol.*, **7**, 195.

GRAY, J., 1955, *J. Exp. Biol.*, **32**, 775.

GRAY, J. and HANCOCK, G. J., 1955, *J. Exp. Biol.*, **32**, 802.

GRAY, J., 1958, *J. Exp. Biol.*, **35**, 96.

HANCOCK, G. J., 1953, *Proc. Roy. Soc.*, **A217**, 96.

Handbook of Biol. Data, 1956, W. S. Spector, editor, Philadelphia, W. B. Saunders Co.

HOFFMAN- BERLING, H., 1955, *Biochim. et Biophysica. Acta.*, **16**, 146.

KAMKE, E., 1948, Differential Gleichungen, New York, Chelsea Publishing Co.

MACHIN, K. E., 1958, *J. Exp. Biol.*, **35**, 796.

MACHIN, K. E., and PRINGLE, J. W. S., 1960, *Proc. Roy. Soc.*, **B152**, 311.

MACHIN, K. E., 1963, *Proc. Roy. Soc.*, **B158**, 88.

MANN, T., 1964, Biochemistry of Semen and the Male Reproductive Tract, New York, John Wiley & Sons, Inc.

MEYER, K. H., and FERRI, C., 1936, *Pfluger's Arch. ges. Physiol.*, **238**, 78.

NELSON, L., 1954, *Biochim. et Biophysica Acta*, **14**, 312.

NELSON, L., 1961, Proceedings of the First International Congress of Histochemistry and Cytochemistry, R. Wegmann, editor, New York, The Macmillan Co.

RIKMENSPOEL, R., 1957*a*, *Experientia*, **13**, 124.

RIKMENSPOEL, R., 1957*b*, Photoelectric and cinematographic observations of the motility of bull sperm cells, thesis, J. A. SMIT, Utrecht.

RIKMENSPOEL, R., VAN HERPEN, G., and EYKHOUT, P., 1960, *Phys. Med. and Biol.*, **5**, 167.

RIKMENSPOEL, R., 1964, *Trans. N. Y. Ac. Sc.*, **8**, suppl., 1072.

RIKMENSPOEL, R., 1965, *Exp. Cell. Research*, **37**, 312.

ROMANOFF, A. L., and ROMANOFF, A. J., 1949, The avian egg, New York, John Wiley & Sons, Inc.

ROTHSCHILD, LORD. 1962, in Spermatozoan Motility, D. W. Bishop, editor, Washington, D. C., American Association for the Advancement of Science.

SOMMERFELD, A., 1947, Theoretische Physik, **2**, Wiesbaden, Dieterlich'sche Verlag.

TAYLOR, G. I., 1952, *Proc. Roy. Soc.*, **A211**, 225.